Indian Journal of Biochemistry & Biophysics
Vol. 60, February 2023, pp. 148-155
DOI: 10.56042/ijbb.v60i2.70710

Design, synthesis, characterization and *in vitro* evaluation of some novel thiol-substituted 1,3,4-oxadiazoles as GlmS inhibitors

Roshan NS[1], Srikanth J[1], Gomathi Swaminathan[1]*, Rebekal J[1], Kannan R[1] & Narasimha Rao G[2]

[1]Department of Pharmaceutical Chemistry; & [2]Department of Pharmacology, JSS College of Pharmacy, JSS Academy of Higher Education & Research, Ooty-643 001, Tamil Nadu, India

Received 28 December 2022; *revised 12 January 2023*

The development of novel medications with previously unidentified action mechanisms is required due to the increasing in antibiotic resistance amongst dangerous microbes. The major goal of the research was to develop *in silico* and *in vitro* antibacterial methods for designing an active thiol substituted oxadiazole inhibitor targeting gram-negative and gram-positive bacteria's GlmS receptor. 1,3,4-Oxadiazole was proposed as a scaffold, and the possibility of its synthesis was examined. The least amount of free energy in the ligand configurations was chosen. Analyses of the novel molecules' characteristics were done using ADMET studies. There were four distinct reactions used in the synthesis processes. As the first reagent, substituted carboxylic acids were utilized. Synthesized compounds were characterized by spectral studies and minimum inhibitory concentration was evaluated by *in vitro* antibacterial examinations of synthesized compounds. Ciprofloxacin served as the study's reference drug. Based on *in vitro* studies and *in silico* molecular docking, ROS1-4 established strong binding energy, while ROS3 revealed significant antibacterial activity. These findings support the hypothesis that the proposed scaffold significantly inhibits the GlmS receptor protein.

Keywords: Antibacterial, GlmS, Molecular docking, Oxadiazole, Spectral studies

Low and lower-middle-income nations like India and Haiti have been reported to be vulnerable against infectious disease although the moralities in these countries have decreased considerably in the above said countries. In 2015 itself 2.74 million deaths were reported due to the cause of various respiratory diseases such as Pneumonia and influenza. Furthermore, Pneumococcal pneumoniae killed in excess to 690,000 people who were aged 70 or more. Also, the number of outbreaks between 2005 and 2009 had increased to almost 3000 cases which comprised of mostly bacteria, viruses and fungi[1]. Lower respiratory infections (3.0 million fatalities), diarrheal illnesses (1.4 million deaths), and tuberculosis (1.3 million deaths) were some of the leading ten mortality causes in 2016. Recent outbreaks of infectious diseases like Ebola, Zika, SARS, Influenza together with the growing antimicrobial resistance (AMR) acquired by different pathogens also makes the road ahead to fight against the various disease-causing microbes challenging. According to World Health Organization (WHO), antimicrobials are classified into three main categories such as critically important, highly important and important based on two criterions of human diseases that is if there is only a sole therapy for one particular disease or if the pathogen acquires resistant genes from non-human sources[2]. The resistant to various antimicrobial agents was always going to become a huge problem like predicted as early as in the 1970s. Particularly, in gram positive bacteria the treatment protocols have never been any harder because of the development of resistant genes from both human and non-human sources[3]. N-acetylglucosamine (GlcNAc) an amino sugar and a vital component in bacterial cell peptidoglycan, chitin, and the extracellular matrix of animal cells. In the first step, glucosamine-6-phosphate synthase (GlmS) using L-glutamine catalyzes the conversion of fructose-6-phosohate (Fru-6-P) to glucosamine-6-phosphate (GlcN-6-P). In several organisms, GlcN6P is a crucial metabolic substrate for a wide range of significant biomolecules (Fig. 1). For instance, GlcN6P plays a role in the manufacture of several glycans in both humans and other mammals, and as a sensing component for glucose absorption in bacteria, it serves as the precursor to the peptidoglycan and lipopolysaccharides that serve as the structural components of their cell walls[4-7]. Related to this, as

*Correspondence:
E-mail: gomathiswaminathan@jssuni.edu.in

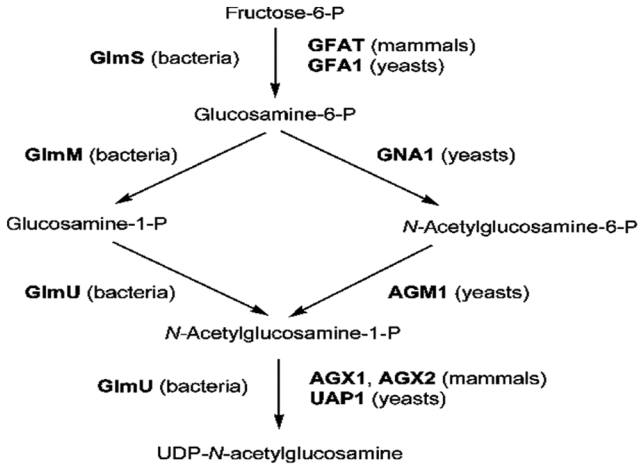

Fig. 1 — Schematic representation of synthesis of UDP-N-acetylglucosamine from Fructose-6-phosphate

GlcN6P is necessary for the production of chitin in fungi, blockers of GlmS also drawn attention[8]. The subsequent step involves phosphoglucose mutase (GlmM), which changes GlcN-6-P into glucosamine-1-phosphate (GlcN-1-P). When GlcN-1-P is converted into N-acetylglucosamine-1-phosphate (GlcNAc1P), which is then proceeded by ultimate product UDP-GlcNAc, the last two consecutive steps of the process involve acetyl transfer with uridyl transfer events. N-acetylglucosamine-1phosphate uridyltransferase (GlmU), a unique bi - functional enzyme with acetyltransferase as well as uridyltransferase activity that is expressed by the glmU gene (Rv1018c), catalyzes both processes. The absence of these enzymes in mammalian counter parts makes these enzymes as an attractive target.

GlmS (Glucosamine-6- Phosphate Synthase) ribozyme needs an exogenous ligand to bind for activity and is the first known example of a natural biocatalyst to exhibit such property. This RNA occurs as a part of the mRNA which encodes the enzyme which synthesize glucosamine 6-phosphate (GlcN6P)[9]. The biochemical process for UDP-N-acetylglucosamine (UDP-GlcNAc) is begin with GlmS enzymes, which change glutamine as well as fructose-6-phosphate in to the GlcN6P & glutamate. That is, a key component of its whole synthetic function is the hydrolytic deamination of glutamine in its glutaminase domain, which results in the production of free ammonia[4]. The former is then transported via a hydrophobic channel to the synthase domain, which is located over 18°. A distant and helps avoid its loss to the solvent[10,11]. The NH_3 reacts with D-fructose 6-phosphate (F6P) in the synthase domain to create GlcN6P. Although it is inhibited by the Q-loop secondary structure, F6P binding in the synthase domain causes the glutaminase domain to bind L-glutamine and the creation of the ammonia channel. However, the tunnel can link because the glutaminase domain is sealed following L-glutamine binding. L-glutamic acid departs initially after the products are produced in both domains, accompanied by glucose-6-phosphate (G6P). Additionally, this stringent regulation prevents the medium from losing ammonia produced by the glutaminase domain (Fig. 1). GlmS is a validated target for the production of antibacterial agents with a broad spectrum of action, and it could be a potential strategy for design of novel antibacterial agents. The current work aims to *in silico* design and synthesize an active thiol substituted oxadiazole derivatives against GlmS receptors of gram-negative and gram-positive bacteria & *in vitro* evaluation of antibacterial properties of synthesized compounds employing gram-negative and gram-positive bacterial strains.

Materials and Methods

Molecular docking[12-17]

The protein *E. coli* glucosamine-6-P synthase (glmS) in complex with glucose-6P and 5-oxo- L-norleucine co-crystals (2J6H.pdb) was downloaded from a PDB database. In the next step, the protein was prepared using free molecular graphics program Swiss-Pdb Viewer[18], where crystal waters, native co-crystal ligands and non-redundant chains were removed. Some missing amino acid residues were added by building loops of Swiss-Pdb Viewer and then subjected to energy minimization using the Gromos force field[19,20]. The protein with the lowest energy constraint was saved in .pdb format and further pre-processed using ADT of AutoDock Tools 1.5.6 program. Pre-processing steps were accomplished via the ADT program, encompassing integration of non-polar hydrogens to the bonded carbon atoms and conveying Kollman charges. The grid was generated using AutoGrid module mapping for each atom type inside the Co-crystal ligand. The dimensions of the grid were 50 × 50 × 50 Å, and it was focused on the centre of mass of the catalytic site of the receptor with a spacing of 0.375 Å. The structures of designed novel ligands were drawn in ChemSketch and using Avogadro software, the energy minimized 3D-strucutures were generated. The lowest energy conformers were selected and were docked into the catalytic pockets of *E. coli* glmS protein keeping ligands and residues in the

pocket flexible. 3D and 2D interactions of the docked ligands were investigated using Discovery Studio Visualizer-20.1.

ADMET studies

The *in silico* pharmacokinetic properties, ADME (absorption, distribution, metabolism and elimination) and toxicity prediction for the synthesized compounds was studied by Data Warrior tool. By identifying substructures of the chemical structural that predicts the toxicity risk within one of the four primary toxicity classes, Data Warrior attempts to evaluate the toxicity risk[21].

General procedure for synthesis of title compounds

As mentioned in the scheme (Fig. 2) the title compounds were synthesized in four steps[22,23].

Step-1: Synthesis of 4-substituted methyl benzoate

A 7 g of 4-substitued benzoic acid was dissolved in excess of methanol (40 mL) with trace amounts of H2SO4 which acts as the proton donor (Fischer's esterification). The mixture was subjected to reflux in the water bath for 4-5 h. The reaction was monitored by TLC with solvent system being n-hexane and petroleum ether in the ratio 1:2. The resulting mixture was subjected to separation using separating funnel with equal amounts of dichloromethane (DCM) and water. After separating out, the unreacted benzoic acid was dissolved in DCM. The solution of water was left to dry out to collect the ester crystals.

Step-2: Synthesis of 4-substituted benzohydrazide

5 g of 4-nitro methyl benzoate was dissolved in 30 mL of ethanol followed by adding 9 mL of 80% hydrazine hydrate and was subjected for reflux in a water bath for 8 h. The light-yellow crystals can be observed to be turning to darker in color as the reaction progresses. The reaction was monitored with TLC with the solvents being ethyl acetate and petroleum ether in the ratio 1:2. After synthesis was finished, the mixture had allowed to cool and solidify into a yellow hydrazide. This was then filtered out to a wattman filter paper and crystalized with ethanol.

Step-3: Synthesis of 5-substituted-1,3,4-oxadizole 2-thiol

To 7 g of 4-substituted benzohydrazide, 40 mL (0.67mol) of ethanol was added and the mixture was diluted.To this 2 mL (0.033mol) of carbon disulfide and a solution of 1.2 g of potassium hydroxide in 20 mL water. The resulting mixture was stirred for 4-6 h until the hydrogen sulfide gas has finished evolving from the reaction vessel. The reaction was monitored with the use of a solvent system of Propanol: n-hexane: Ethyl acetate in the ratio of 2.5:1.5:1.

Step-4: General procedure for the synthesis of 4-nitro"-N'-({[5-substituted-1,3,4-oxadiazol-2-yl]sulfanyl}acetyl) benzohydrazide

Equal moles of both the hydrazide compounds and the oxadiazole derivatives were taken. The hydrazide derivative compounds were added along with 1.5 equivalents of activated K2CO3. The mixture was stirred in prepared dry acetone. After a time period of 1 h, 1 equivalent of 5-substituted-1,3,4-oxadizole 2-thiol was added, then stirred for 24-48 h. The reaction was monitored with the use of a solvent system of ethyl acetate and petroleum ether in the ratio 1:2. The resulting compound was crystallized using methanol as solvent. The physical properties of the final synthesized compounds ROS1-4 were mentioned in the (Table 1).

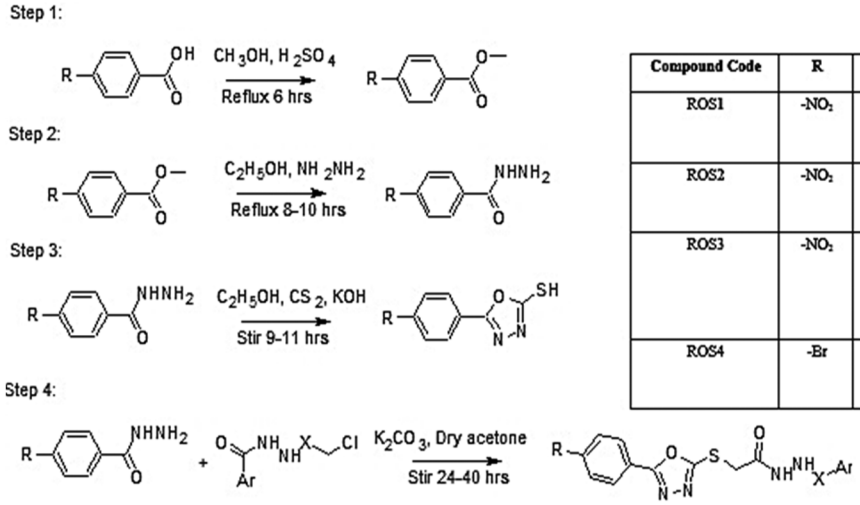

Compound Code	R	Ar	X
ROS1	$-NO_2$		-C=O
ROS2	$-NO_2$		$-SO_2$
ROS3	$-NO_2$		-C=O
ROS4	-Br		-C=O

Fig. 2 — Scheme for the synthesis of title compounds (ROS_{1-4})

Table 1 — Physical properties for the synthesized compounds ROS_{1-4}

Compound code	Structure	Molecular formula	Molecular weight (g/mol)	Melting point (°C)	R_f value
ROS1	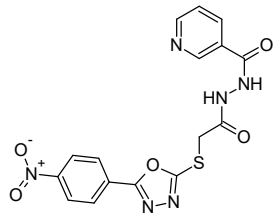	$C_{16}H_{12}N_6O_5S$	400.36	243-248	0.65
ROS2	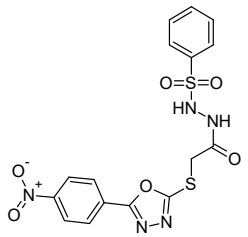	$C_{16}H_{13}N_5O_6S_2$	435.43	238-242	0.69
ROS3	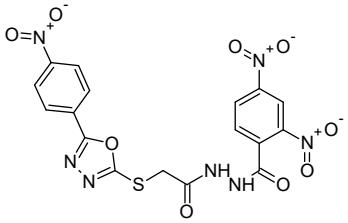	$C_{17}H_{11}N_7O_9S$	489.37	215-221	0.43
ROS4	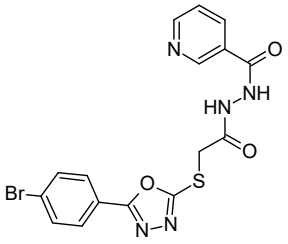	$C_{16}H_{12}BrN_5O_3S$	434.26	282-285	0.52

***In vitro* Anti-bacterial activity**

Minimum Inhibitory Concentration (MIC) studies

As per the CLSI guidelines the MIC of synthesized compounds were studied using the micro-broth dilution process. The test substances were examined using a panel of Gram-negative bacteria and Gram-positive bacteria at concentrations ranging from 7.8 to 250 µg/mL. Two strains of Gram-positive bacteria employed in the study were *S. aureus* (NCIM 5021) and MRSA (NCIM 43300). Whereas, two strains of Gram-negative bacterial were *K. pneumoniae* (NCIM 2706) and *P. aeruginosa* (NCIM 5032). The MIC values of synthesized novel compounds were related with the standard antibiotic Ciprofloxacin[24,25].

Results and Discussion

Molecular docking

The molecular docking of the designed compounds was done by the employing Autodock 4.2 software[26]. A dataset of 200 ligands were designed by linking 5-phenyl-2-Thiol-oxadiazole ring with different substituted carboxylic acid and sulfono hydrazides. Most of the docked compounds displayed interactions with similar catalytic pocket amino acids. The binding energy values (Table 2) for the designed ligands was in the range of −8.3 to −10.2 kcal/mol, when compared with substrate glucose-6-phosphate (−10.1 kcal/mol). The docked compounds exhibited hydrogen bonding interactions with Glu301, Thr302,

Table 2 — Binding energy values (kcal/mol) for the synthesized compounds ROS_{1-4} in the catalytic pocket of *E. coli* glucosamine-6-P synthase (glm S) (2J6H.pdb)

Compound	Binding energy (kcal)	Interacting residues
G6P	-10.2	Asn305, Leu484, Leu480, Ala496, Glu495
ROS1	-9.2	Leu484, Leu480, Ala496, Glu495
ROS2	-9.4	Thr302, Asn305, Leu484, Leu480, Glu495
ROS3	-10.1	Thr302, Ser349, Glu488, Lys603
ROS4	-9.5	Thr302, Asn305, Ser349, Leu484, Leu480

Ser303, Asn305, Gln348, Ser349, Leu480, Leu484, Lys487, Glu495, Ala496, Tyr497 and Lys603. The top scored ROS3 showed significant binding energy (−10.1 kcal/mol) by forming hydrogen bonds with Thr302, Ser349 and Lys603 (Fig. 3).

ADMET studies

ADMET properties of all the synthesized compounds were evaluated using Data warrior (Table 3). Various properties like cLogP, cLogS were analyzed to evaluate the lipophilic property of the individual drugs which is key in the absorptive properties of any drug molecule. Other properties like hydrogen bond acceptors and hydrogen bond donors were also evaluated to check the adherence to the Lipinski's rule.

Chemistry

The complete synthetic route chosen to synthesize the designed compounds have been illustrated in the (Fig. 2). In the first step, different derivatives if benzoic acid (4-nitro and 4-bromo) were opted to undergo Fischer's etherification wherein the carboxylic group gets converted into an ester group upon addition of a methyl group. The benzoic acids were reacted with excess methanol because the reaction being chemically equilibrium in nature. The solution was also provided with enough hydrogen ions to carry out the reaction under reflux at 100°C. The formation of ester was noted by the fruity smell the product accompanies. The ester is then subjected to reflux with hydrazine hydrate to form the hydrazide derivative along with ethanol as the solvent. The hydrazide was yellow-brown in color for both the derivatives. The excess ammonia resultant from the reaction is discarded and the product is purified.

The next step involves the ring formation or cyclisation which ultimately leads to oxadiazole formation. The thionylating agent of the reaction being CS2. The KOH was also necessary for the progress of the reaction. The reaction was run for approximately 4-6 h under reflux and constant stirring. The evolving of H2S gas indicates the progression of the reaction which has a pungent smell to it. The reaction was observed to be finished when all of the Hydrogen sulfide gas has stopped evolving from the reaction mixture. The reaction was also monitored by TLC. The product was then subjected to condensation with various derivatives. The condensation reaction usually lasts for about 24-48 h.

The reaction was carried out with the solvent being dry acetone. The dry acetone was prepared by refluxing acetone with potassium permanganate and then distilling with activated potassium carbonate (120°C). The reaction mixture was also further added with 1.5 eq of Potassium carbonate to eliminate any possible water content. The reaction was monitored with TLC. The synthesized compounds were characterized with spectral data such as IR, NMR and MASS spectra. The IR band of -NH- and -NH-NH- are observed in the region of 3060-3300 cm^{-1}. The characteristic band of -C=O- in an amide was observed in the range of 1600-1680cm^{-1}. The -C-Br- band was observed in the region of 668cm^{-1}. The formation of –S-CH2- linker was observed by appearance of signals at 4.66-3.29 ppm in 1H NMR and 67.46-53.23 ppm in 13C NMR.

4-nitro-N'-({[5-(4-nitrophenyl)-1,3,4-oxadiazol-2-yl]sulfanyl}acetyl)benzohydrazide (ROS1): Solvent crystallization: Methanol; Yield 65%; m.p=243-248°C; Rf =0.65; IR (KBr) (cm-1)v: 3172, 3120 (NH), 3063 (C=C), 1694 (>C=O), 1107 (C-O-C), 1662 (C=N), 3084 (Ar C-H) 1510 (N-O); 1H-NMR (DMSO-d6): δppm 10.53 (s, 1H, NH), 10.49 (s, 1H, NH), 8.49-8.02 (m, 4H, ArH), 7.72-

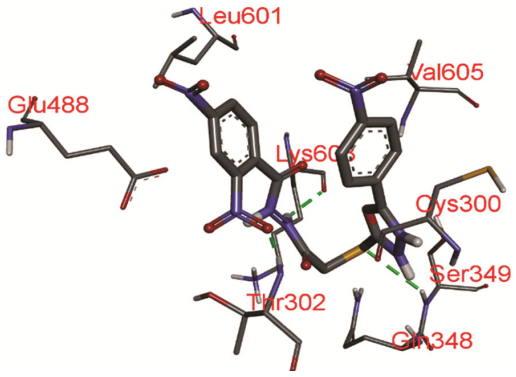

Fig. 3 — 3D docking pose of ROS3 in the catalytic pocket of *E. coli* glucosamine-6-P synthase (glm S) (2J6H.pdb)

Table 3 — ADMET properties for the synthesized compounds ROS_{1-4} calculated with Data warrior

Compound	cLogP	cLogS	H-Acceptors	H-Donors	Total Surface Area	Relative PSA	Polar Surface Area	Druglikeness
ROS1	0.054	-6.27	13	2	317	0.515	214.06	-2.19
ROS2	0.051	-4.005	11	2	304.16	0.488	193.69	-15.02
ROS3	0.772	-6.158	15	2	322.92	0.559	242.81	-2.19
ROS4	1.621	-5.389	8	2	287.05	0.395	135.31	1.09

Table 4 — MIC values (µg/mL) for the synthesized compounds ROS_{1-4} against selected bacterial strains

Compound	*S. aureus* (NCIM 5021)	MRSA (NCIM 43300)	*K. pneumoniae* (NCIM 2706)	*P. aeruginosa*(NCIM 5032)
ROS1	43.41	117.46	3.90	91.47
ROS2	6.09	288.09	8.78	145.70
ROS3	3.80	4.77	7.56	9.20
ROS4	2.22	162.19	59.63	77.65
Ciprofloxacin	1.01	209.24	27.24	73.89

7.49 (m, 4H, ArH), 4.66 (s, 2H, SCH2); 13C-NMR spectrum (DMSO-d6): δppm 185.66 (>C=O), 166.86, 152.07, 143.55, 131.16, 130.29, 129.39, 122.96, 118.47, 117.38, 66.47 (SCH2). MS (ESI) *m/z*: calculated for C16H12N6O5S (400.36). Found: *m/z* 400.3.

N'-(benzenesulfonyl)-2-{[5-(4-nitrophenyl)-1,3,4-oxadiazol-2-yl]sulfanyl}acetohydrazide(ROS2): Solvent crystallization: Methanol; Yield 70%; m.p=238-242°C; Rf=0.69 IR (KBr, cm-1) v:3265 (NH), 3052 (Ar C-H), 2936 (CH2), 1693 (>C=O), 1511(NO2), 1412 (S=O), 1654 (C=N); 1H-NMR (DMSO-d6): δppm 10.48 (s, 1H, NH), 10.12 (s, 1H, NH), 8.89-8.19 (m, 5H, ArH), 7.88-7.79 (m, 4H, ArH), 4.81 (s, 2H, SCH2); 13C-NMR spectrum (DMSO-d6): δppm 171.26 (>C=O), 164.32, 160.52, 155.07, 142.25, 131.06, 130.48, 122.46, 118.17, 67.46 (SCH2).MS (ESI) *m/z*: calculated for C16H13N5O6S2 (435.437). Found: *m/z* 435.3.

N'-(2,4-dinitrophenyl)-2-{[5-(4-nitrophenyl)-1,3,4-oxadiazol-2-l]carbonyl}acetohydrazide (ROS3): Solvent crystallization: Methanol; Yield 66 %; m.p=215-221°C; Rf=0.43. IR (KBr) (cm-1) v: 3247 (NH), 3068 (Ar C-H), 1675 (>C=O), 1650 (C=N), 1540 (NO2). 1H-NMR (DMSO-d6): δppm 10.33 (s, 1H, NH), 10.27 (s, 1H, NH), 7.96-7.29 (m, 3H, ArH), 7.18- 6.67 (m, 4H, ArH), 3.39 (s, 2H, SCH2); 13C-NMR spectrum (DMSO-d6): δppm 181.26 (>C=O), 168.16 (>C=O), 152.80,151.36, 131.53, 129.67, 126.23, 125.23, 124.23, 118.63, 68.85, 53.23 (SCH2). MS (ESI) m/z: calculated for C16H13N5O6S2 (444.4343). MS (ESI) *m/z*: calculated for C17H11N7O9S (489.377). Found: *m/z* 489.3.

N'-({[5-(4-bromophenyl)-1,3,4-oxadiazol-2-yl]sulfanyl}acetyl)pyridine-3-carbohydrazide (ROS4): Solvent crystallization: Methanol and n-hexane: DCM (1:3:7).Yield 50 %; m.p=282-285°C; Rf=0.52; IR (KBr) (cm-1) v: 3247 (NH), 3084 (Ar C-H), 1682 (>C=O), 1650 (C=N),1550 (NO2), 668(C-Br). 1H-NMR (DMSO-d6): δppm 10.53 (s, 1H, NH), 10.37 (s, 1H, NH), 7.92-7.29 (m, 4H, ArH), 7.18-6.17 (m, 4H, ArH), 3.29 (s, 2H, SCH2); 13C-NMR spectrum (DMSO-d6): δppm 186.26 (>C=O), 166.36 (>C=O), 151.80,150.36, 132.53, 128.67, 126.23, 125.23, 118.63, 68.85, 53.33 (SCH2). MS (ESI) *m/z*: calculated for C16H12BrN5O3S (434.263). Found: *m/z* 436.3 (M++).[27]

***In vitro* Anti-bacterial activity**

Minimum Inhibitory Concentration (MIC) studies

As per the CLSI guidelines we evaluated the MIC activity of synthesized compounds using the micro-broth serial dilution process. The test compounds were screened against a panel of Gram-negative and Gram-positive bacteria at concentrations ranging from 7.8 to 250 µg/mL. The strains included half Gram-negative and half gram-positive bacteria which consisted of *S. aureus* (NCIM 5021), *MRSA* (NCIM 43300), *K. pneumoniae* (NCIM 2706) and *P. aeruginosa* (NCIM 5032).The findings were compared to the standard antibiotic Ciprofloxacin, and the results were summarized in the (Table 4). From the MIC studies, it is evident that all the synthesized compounds exhibited moderate inhibition potency which was comparable to standard drug (ciprofloxacin). Out of all the compounds, among all the examined bacterial strains, ROS3 demonstrated the strongest antibacterial activity. The ROS3 showed more pronounced antibacterial activity against the resistant strain of MRSA (43300) with a MIC of 4.77 µg/mL far bettering the MIC of the standard which was 209.24 µg/mL. Also all of the synthesized compounds, except ROS4 showed better inhibitory concentration (3.90-7.56 µg/mL) against *K.pneumoniae* (NCIM 2706[28-30].

Conclusion

The protein E. coli glucosamine-6-P synthase (glmS) obtained from the RSC-PDB database (2J6H.pdb) was prepared and molecular docking was performed for the designed thiol-substituted 1,3,4-oxadiazoles linked with substituted carboxylic acid and sulfono hydrazides. From molecular docking analysis, based on the hydrogen bonding and binding energy values the first four compounds were synthesized and spectral characterization was done.

The binding energy values for the designed ligands was in the range of −8.3 to −10.2 kcal/mol, when compared with substrate glucose-6-phosphate (−10.1 kcal/mol). The top scored ROS3 showed significant binding energy (−10.1 kcal/mol) by forming hydrogen bonds with Thr302, Ser349 and Lys603. ADMET properties of all the synthesized compounds were evaluated using Data warrior. Various parameters like cLogP, cLogS, hydrogen bond acceptors and hydrogen bond donors were analyzed to check the adherence to the Lipinski's rule. From the MIC studies, it is evident that all the synthesized compounds exhibited moderate inhibition potency when compared to standard drug ciprofloxacin. The compound ROS3 showed the most significant antibacterial activity against all the tested bacterial strains, where, ROS3 showed more pronounced antibacterial activity against the resistant strain of MRSA (43300) with a MIC of 4.77 µg/mL far bettering the MIC of the standard. Also all of the synthesized compounds, except ROS4 showed better inhibitory concentration (3.90-7.56 µg/mL) against *K. pneumoniae* (NCIM 2706). On the basis of *in silico* molecular docking and *in vitro* studies ROS1-4 showed good binding energy and ROS3 exhibited significant anti-bacterial activity. Further studies will be needed to establish the antibacterial mechanism and its relation with the pharmacophoric features.

Conflict of interest

All authors declare no conflict of interest.

References

1 Jen Christiansen 2018, Global Infections by the Numbers-Scientific American. [ONLINE] Available at: https://www.scientificamerican.com/article/global-infections-by-the-numbers/ [Accessed 01 May 2018].

2 WHO 2019, Critically important antimicrobials for human medicine, 6th revision. Available at: https://www.who.int/publications/i/item/9789241515528 [Accessed 20 March 2019].

3 Aksoy DY & Unal S, New antimicrobial agents for the treatment of Gram-positive bacterial infections. *Clin Microbiol Infect*,14 (2008) 411.

4 Teplyakov A, Obmolova G, Badet-Denisot MA & Badet B, The mechanism of sugar phosphate isomerization by glucosamine 6-phosphate synthase. *Protein Sci,* 8 (1999) 596.

5 Khan MA, Göpel Y, Milewski S & Görke B, Two small RNAs conserved in enterobacteriaceae provide intrinsic resistance to antibiotics targeting the cell wall biosynthesis enzyme Glucosamine-6-Phosphate synthase. *Front Microbiol*, 7 (2016) 908.

6 Bearne SL & Blouin C, Inhibition of *Escherichia coli* glucosamine-6-phosphate synthase by reactive intermediate analogues: The role of the 2-amino function in catalysis. *J Biol Chem,* 275 (2000) 135.

7 Bearne SL, Active site-directed inactivation of *Escherichia coli* glucosamine-6-phosphate synthase: Determination of the fructose 6-phosphate binding constant using a carbohydrate-based inactivator. *J Biol Chem*, 271 (1996) 3052.

8 Wojciechowski M, Milewski S, Mazerski J & Borowski E. Glucosamine-6-phosphate synthase, a novel target for antifungal agents: Molecular modelling studies in drug design. *Acta Biochim Pol,* 52 (2005) 647.

9 Ferre-DAmaré AR, The glmS ribozyme: use of a small molecule coenzyme by a gene-regulatory RNA. *Q Rev Biophys*, 43 (2010) 423.

10 Mouilleron S, Badet-Denisot MA, Badet B & Golinelli-Pimpaneau B, Dynamics of glucosamine-6-phosphate synthase catalysis. *Arch Biochem Biophys,* 505 (2011) 1.

11 Floquet N, Mouilleron S, Daher R, Maigret B, Badet B & Badet-Denisot MA, Ammonia channeling in bacterial glucosamine-6-phosphate synthase (Glms): molecular dynamics simulations and kinetic studies of protein mutants. *FEBS Lett,* 581 (2007) 2981.

12 Richa Kothari, Anurag Agrawal & Sanchita Rai, Molecular docking and Antibacterial activities of Cobalt (II) complexes derived from precursors of Hydrazones. *Indian J Biochem Biophys,* 59 (2022) 640.

13 Toppo AL, Yadav M, Dhagat S, Ayothiraman S & Eswari JS, Molecular docking and ADMET analysis of synthetic statins for HMG-CoA reductase inhibition activity. *Indian J Biochem Biophys,* 58 (2021) 127.

14 Dash S, Ishani I, Lahiri D & Nag M, Evaluation of predictive machine learning models for drug repurposing against delta variant of SARS-CoV-2 spike protein. *Indian J Biochem Biophys,* 59 (2022) 879.

15 Agrawal A, Kulkarni GT & Lakshmayya, Molecular docking study to elucidate the anti-pruritic mechanism of selected natural ligands by desensitizing TRPV3 ion channel in Psoriasis: An *in silico* approach. *Indian J Biochem Biophys,* 57 (2020) 578.

16 Mishra AK, Gupta V & Tewari SP, *In silico* screening of some naturally occurring bioactive compounds predicts potential inhibitors against SARS-CoV-2 (COVID-19) protease. *Indian J Biochem Biophys*, 58 (2021) 416.

17 Fathima Shahana M & Yardily A, Synthesis, quantification, dft Calculation and molecular docking of (4-amino-2-(4-methoxyphenyl)aminothiazol-5yl)(thiophene-2-yl)methanone. *Indian J Biochem Biophys,* 57 (2020) 606.

18 Kaplan W & Littlejohn TG, Swiss-PDB Viewer (Deep View). *Brief Bioinform,* 2 (2001) 195.

19 Bachmann SJ & van Gunsteren WF, On the compatibility of polarisable and non-polarisable models for liquid water. *Mol Phys,* 112 (2014) 2761.

20 Hansen N, Heller F, Schmid N & van Gunsteren WF, Time-averaged order parameter restraints in molecular dynamics simulations. *J Biomol,* 60 (2014) 169.

21 Lajiness MS, Vieth M & Erickson J, Molecular properties that influence oral drug-like behavior. *Curr Opin Drug Discov Devel,* 7 (2004) 470.

22 Almajan GL, Barbuceanu SF, Saramet I, Dinu M, Doicin CV & Draghici C, Synthesis and biological evaluation of various new substituted 1,3,4-oxadiazole-2-thiols. *Revista de Chimie,* 59 (2008) 395.

23 Batool M, Tajammal A, Farhat F, Verpoort F, Khattak ZAK, Mehr-un-Nisa, Shahid M, Ahmad HA, Munawar MA, Zia-Ur-Rehman M & Basra MAR, Molecular docking, computational, and antithrombotic studies of novel 1,3,4-oxadiazole derivatives. *Int J Mol Sci,* 19 (2018) 3606.

24 Bhat B, Vaid S, Habib B & Baja BK, Design of experiments for enhanced production of bioactive exopolysaccharides from indigenous probiotic lactic acid bacteria. *Indian J Biochem Biophys,* 57 (2020) 539.

25 Singh R, Prasad J, Satapathy T, Jain P & Singh S, Pharmacological evaluation for anti-bacterial and anti-inflammatory potential of polymeric microparticles. *Indian J Biochem Biophys,* 58 (2021) 156.

26 Morris GM, Huey R, Lindstrom W, Sanner MF, Belew RK, Goodsell DS & Olson AJ, AutoDock4 and AutoDockTools4: Automated docking with selective receptor flexibility. *J Comput Chem*, 30 (2009) 2785.

27 Singh S, Synthesis, spectroscopic studies and pesticidal activity of transition metal complexes with unsymmetrical schiff base. *Indian J Biochem Biophys*, 58 (2021) 565.

28 Kowalska-Krochmal B & Dudek-Wicher R, The minimum inhibitory concentration of antibiotics: methods, interpretation, clinical relevance. *Pathogens,* 10 (2021) 165.

29 Andrews JM, Determination of minimum inhibitory concentrations. *J Antimicrob Chemother,* 48 (2001) 5.

30 Wiegand I, Hilpert K & Hancock REW, Agar and broth dilution methods to determine the minimal inhibitory concentration (MIC) of antimicrobial substances. *Nat Protoc*, 3 (2008) 163.